DSM GENERATION FROM EARLY ALOS/PRISM DATA USING SAT-PP

K. Wolff, A. Gruen

Institute of Geodesy and Photogrammetry, ETH-Zurich, CH-8093 Zurich, Switzerland
<wolff><agruen>@geod.baug.ethz.ch

KEY WORDS: PRISM images, high resolution, image matching, DSM generation, validation

ABSTRACT:

The new Japanese optical sensor ALOS/PRISM which was launched in January 2006 has stereo capabilities which can be used for a great number of applications and products. One of the most important products is the generation of Digital Surface Models (DSMs). With SAT-PP (Satellite Image Precision Processing) our group has developed a suite of new methods and a software package which can be used for the 3D processing of optical Linear Array CCD – based satellite sensor systems. The software was already used successfully for the DSM generation with e.g. IKONOS, QuickBird and SPOT5 high resolution image data. Here we will demonstrate the functionality of the automated image matcher for the generation of DSMs by using early ALOS/PRISM data with a ground sampling distance of 2.5 meters.
We have tested our methods of DSM generation using the ALOS/PRISM dataset of two different testfields, which are located in the areas of Bern/Thun (Switzerland) and Okazaki (Japan). They have different topography and land use features (mountainous, city, forest, open and mixed areas). For a detailed quality control of the DSM generation, reference data for three sub areas of the testfield Bern/Thun were available and one sub area in Okazaki. A detailed analysis is presented for certain areas with special and homogeneous topography or land use characteristics. The overall height RMSE for the three sub-areas was 2-3 pixels depending primarily on surface roughness, vegetation and image texture and image quality. The height RMSE values for the specific areas ranged from less than 2 pixels (open areas) to 5 pixels in a tree-covered area.
ALOS/PRISM images have particular radiometric problems which do not influence the final results significantly, but they can influence the DSM generation locally. Therefore we give also an analysis of image artifacts.

1. INTRODUCTION

Digital Surface Model (DSM) generation is one of the most important products of optical image data processing. In recent years CCD Linear Array sensors like IKONOS, QuickBird and, to a lesser extent, also ALOS/PRISM, were and still are widely used to acquire high-quality, high-resolution panchromatic and multispectral image data for photogrammetric and remote sensing applications. To generate high-quality DSMs from this kind of data, efficient approaches are required. Our group has developed the software package SAT-PP (Satellite Image Precision Processing) for the precision processing of high-resolution satellite image data (Gruen et al., 2005). The main module of the package is the automated image matcher for the generation of DSMs (Zhang, 2005). This paper demonstrates its functionality and presents the results of our work as a Member of JAXA's Calibration/Validation Team for processing early ALOS/PRISM image data.
The image matching approach for automatic DSM generation from Linear Array sensors developed in SAT-PP has the ability to provide dense, precise and reliable results. The approach uses a coarse-to-fine hierarchical solution with an effective combination of several image matching algorithms for multiple views and automatic quality control. To improve the matching results image pre-processing with the Wallis filter is realized.
For the evaluation of DSM generation with SAT-PP and ALOS/PRISM image data we used two image triplets, one shows the area around Bern/Thun in Switzerland and the other the area around Okazaki in Japan. For a detailed analysis we defined sub areas with special and homogeneous topography or land use characteristics.
Although the images have particular radiometric problems, the required sensor orientation and matching results are at a good level of accuracy. No manual post-correction of the generated DSMs was done. The RMS errors for the four main test areas are between 5.5 m to 6.6 m, which means better than three pixels. As expected, we got the best results in open terrain (RMS height error better than two pixels) and the worst in tree-covered areas (RMS height errors between three and five pixels). For details of the sensor orientation and its results see (Gruen et al., 2007) and (Kocaman and Gruen, 2007).
First we describe the methods used in the matching module of SAT-PP and the procedure of the evaluation of the DSM generation. ALOS/PRISM images have particular radiometric problems, which do not influence the final results significantly, but they can influence the DSM generation locally. Therefore we give an analysis of image artifacts and the resulting artifacts in the DSMs. Then we give the results of the quality control of the DSM generation using data from both testfields. For each testfield, we give a short description, the results of the quality control and a final discussion.

2. METHODS

2.1 DSM generation using SAT-PP

The powerful software package SAT-PP can accommodate images from ALOS, IKONOS, QuickBird, SPOT5 HRG/HRS, Cartosat-1 and sensors of similar type to be expected in the future. For a detailed documentation of the software package and the underlying algorithms see (Gruen et al., 2005, Zhang, 2005; Zhang and Gruen, 2004; Zhang and Gruen, 2006).

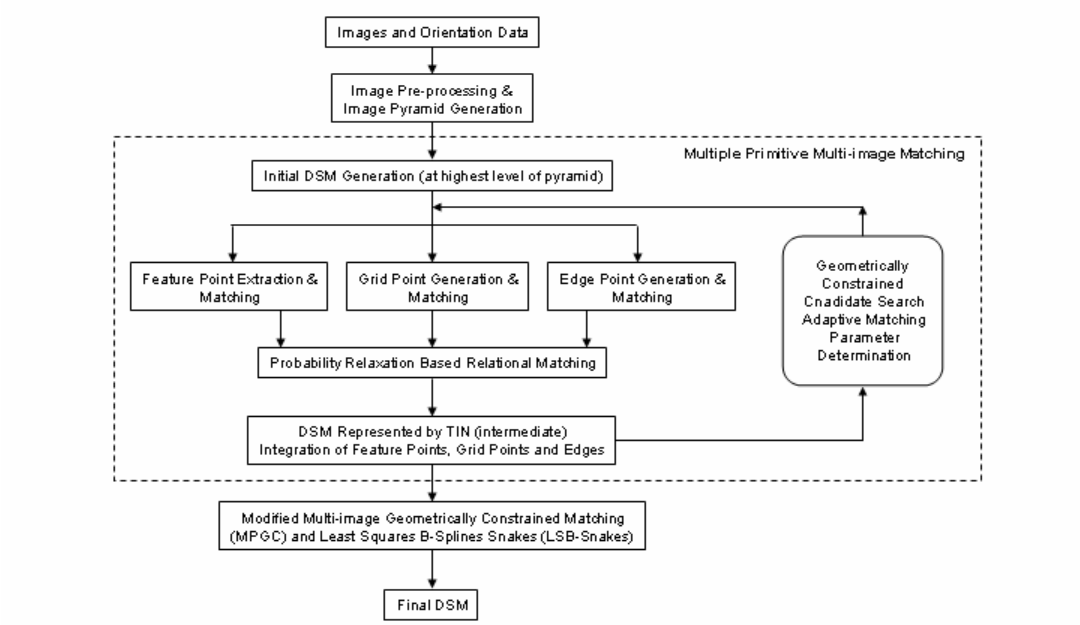

Figure 1. Work-flow of the automated DSM generation approach

The main component of the software package is the matching algorithm for the DSM generation. The procedure is based on a multi-image Least-Squares Matching (LSM) for image features like points and lines. The image matching approach uses a coarse-to-fine hierarchical solution with an effective combination of several image matching methods and automatic quality indication. In addition to the multi-image processing of Linear Array CCD images, the approach is also applicable to single frame aerial photos (analog and digital).

The whole system mainly consists of three mutually connected sub-systems:

1) *The image preprocessing module*, to reduce the effects of the radiometric problems and optimize the images for subsequent feature extraction and image matching.

2) *The multiple primitive multi-image (MPM) matching module*, to get approximations for the refined matching module.

3) *The refined matching module*, in which least squares matching methods are used to achieve more precise matches for all features and identify some false matches.

The overall data flow of the matching approach is shown schematically in Figure 1. The input for the DSM generation are the two or more images and the given or previously triangulated orientation elements. First the software pre-processes the images using a combination of an adaptive smoothing filter and the Wallis filter. The adaptive smoothing filter reduces the noise level, while sharpening edges and preserves even fine details such as corners and line end-points. The Wallis filter is used to strongly enhance the already existing texture patterns. The noise has been already reduced, therefore it is not enhanced by the Wallis filter. After pre-processing and production of the image pyramids, the matches of three kinds of features, here feature points, grid points and edges, on the original resolution images are found progressively starting from the low-density features on the images with the low resolution. Matching with edges and feature points alone may provide under certain conditions very sparse matching results. Therefore, SAT-PP uses also uniformly distributed grid points for matching.

Multi-image matching in object space is a reasonable solution to reduce problems caused by occlusions, multiple solutions and surface discontinuities. A coarse-to-fine hierarchical approach, combined with efficiently implementation of the epipolar geometry and the piecewise smoothness surface constraint, was found to be very important in order to control the computational complexity and to ensure a high reliability for the final matched results.

A combined matching process (point matching, edge matching and a relaxation based relational matching process) goes through all the image pyramid levels in the MPM matching module and generates very good approximations for the refined matching module.

A TIN is reconstructed from the original point cloud of the matched features on each level of the pyramid using the constrained Delauney triangulation method, which in turn is used on the subsequent pyramid level for the approximations and adaptive computation of the matching parameters.

The least squares matching, as an option, is only performed on the original resolution images. Here, the modified MultiPhoto Geometrically Constrained (MPGC) matching method is used for point matching while a Least Squares B-Spline Snakes (LSB-Snakes) is used for matching edges, which are represented by parametric linear B-Splines in object space.

Water areas like wide rivers and lakes can be defined in SAT-PP as so-called dead areas. Also, disturbing objects like clouds or image artifacts can be defined likewise and excluded from matching.

For visualization purposes SAT-PP has also the possibility to assign to these areas a fixed height (see Figure 2).

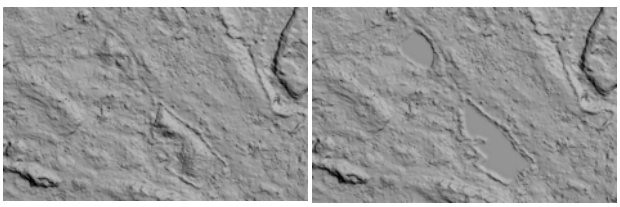

Figure 2. Defining lakes as water areas with a fixed height for visualization. Left: The two lakes were not defined as water areas and appear as small hills. Right: The two lakes with a fixed height.

2.2 DSM generation with ALOS/PRISM

For the DSM generation ALOS/PRISM image triplets of each testfield were available. As orientation elements we used rational polynomials coefficients (RPCs). The given RPCs for the ALOS/PRISM images are not accurate enough to get a high-quality DSM. Because of this, we determined more accurate RPCs by ourselves using parameters of self-calibration based on our DGR georeferencing model. For the determination of the parameters of this rigorous model see (Gruen et al., 2007) and (Kocaman and Gruen, 2007).
We defined all significant lakes as dead areas without any prior height information. For the visualization of the generated DSMs we have chosen a shaded representation.

2.3 Realization of the DSM quality control

For the DSM quality control we compared the generated DSMs with given reference DSMs, having an accuracy of higher order.
For our tests, all reference DSMs (REF) and the generated DSMs (GEN) were given at the same grid points. Therefore the comparison of the two DSMs could be realised by a calculation of the vertical differences between them for each point. As a quality degree we determined the Root Mean Square height Error $(RMSE_Z)$ of all n points by using the following equation:

$$RMSE_Z = \sqrt{\frac{\sum_{i=1}^{n}(Z_{GEN,i} - Z_{REF,i})^2}{n}}$$

The details of a terrain can have a different degree of complexity. Objects on the terrain and the terrain itself in urban or suburban areas have a quite different appearance from those in forest or open rural areas. The difficulties are increased by the facts that many features are similar to each other, homogeneous areas are frequent, large surface discontinuities are common and moving objects may disrupt the images. All this influences directly the quality of automated surface reconstruction from large-scale images. To distinguish between the qualities for these different terrain types, we subdivided the testfields in certain areas with special and homogeneous topography or land use characteristics and computed quality control measures for the whole testfield and for each sub area separately.

Figure 3. Example for radiometric problems with black reference calibration, resulting in striping.

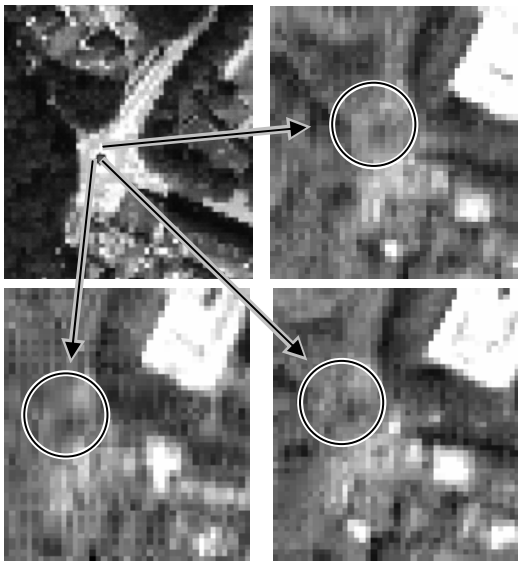

Figure 4. Radiometric problems like jpeg artifacts and striping make the detection of GCPs (here a traffic circle) in image space difficult. Upper left: An image patch from an aerial photo at the same spatial resolution.

3. IMAGE DATA

Early ALOS/PRISM images do have in general radiometric quality problems, leading to image artifacts, partially to fixed pattern noise. The reasons for those deficiencies are problems with black reference calibration (resulting in striping), jpeg-compression (resulting in blocking), saturation effects (mainly related to only 8-bit radiometric depth collection) and others. These problems can influence in a negative way the measurements of GCPs and check points for georeferencing and the image matching for DSM generation. In the following we give some examples.

Figure 3 shows an example for radiometric problems with black reference calibration, resulting in vertical striping.

Figure 4 shows this effect on measuring a GCP which is defined by the centre of a traffic circle. The image top left shows a cutout of an aerial image of the traffic circle with the same resolution like the original ALOS/PRISM image triplet.
The traffic circle gets almost lost in the PRISM image patches. Obviously, it is not possible to measure the GCP even with pixel accuracy.

Figure 5 shows a horizontal line artifact in image space and the resulting artifact in object space. The stripe in image space is more than 10 pixels wide. Such areas should be defined in the affected image as dead areas and should not be used for DSM generation.

Figure 6 gives another example of the influence of radiometric quality on the DSM generation. The triplet shows a flat area with different fields. The textures of the fields look different for each view of the triplet. In the upper part of all images jpeg artifacts are also visible. The differences of the radiometry between the triplet images lead to an error in the generated DSM of more than 10 pixels (25 m), shown in the lower right image.

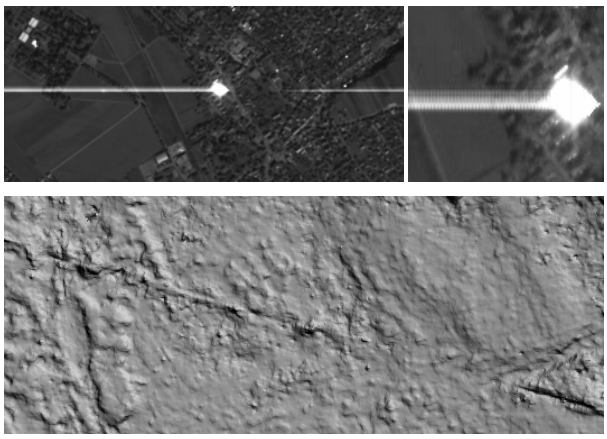

Figure 5. Image artifacts (light line of 13 pixels width across flight direction, upper image), leading to artifacts also in the DSM (diagonal line, lower image).

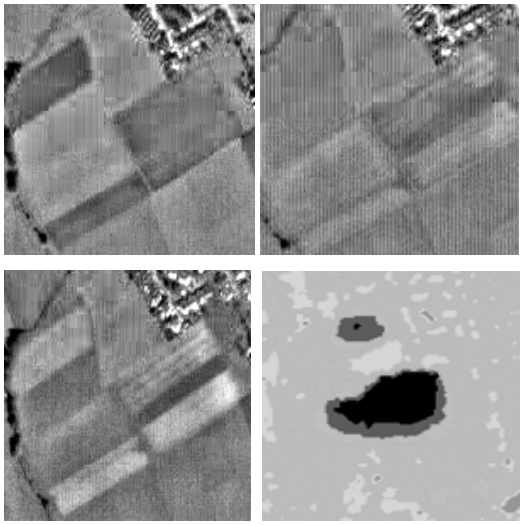

Figure 6. Radiometric differences between the triplet images and the resulting error (grey value coded) in the generated DSM. The dark area indicates an error of more than 25 m.

4. RESULTS

4.1 Testfield Bern/Thun, Switzerland

The Bern/Thun testfield is placed between the two Swiss cities Bern and Thun. It contains beside the two cities different terrain types like a mountainous region in the southern part, smooth hilly regions, open areas, forests, two rivers and the Lake of Thun. A smaller part of the DSM around Thun was already used previously for the evaluation of IKONOS imagery (Eisenbeiss et al., 2004). The testfield in its current form and the GCP field were set up by our group under a contract with JAXA. The coordinates of the GCPs were determined by GPS.
For the validation of the sensor model of PRISM we used the whole area, for the validation of the DSM generation we used three smaller parts (see below). For the generation of the three reference DSMs we made use of aerial images of scale 1:25 000 to 1:34 000 and our software package SAT-PP. We defined the rivers and bigger lakes as dead areas without any given height. The expected accuracy of the DSMs is in the range of 0.5 m to 2.5 m and is therefore by a factor 5 better than the expected PRISM matching results (see Gruen et al., 2006).
Table 1 gives the main parameters of the PRISM dataset acquired over the Bern/Thun testfield.The generated DSM without any manual correction is shown in Figure 7 together with the areas of the three DSM testfields. The grid spacing is 5 m (2 pixels). We evaluated the DSM accuracy for each testfield separately and also for different sub-areas with special topographic or land use features (open areas, city areas, forest and alpine areas).

Table 1. Main parameters of the PRISM dataset acquired over the Bern/Thun testfield

Testfield Bern/Thun, Switzerland	
Imaging date	Sept. 21, 2006
Number of used GCPs	25
$RMSE_{XY}$ of self-calibration (DGR)	1.8 m
$RMSE_{Z}$ of self-calibration (DGR)	1.46 m

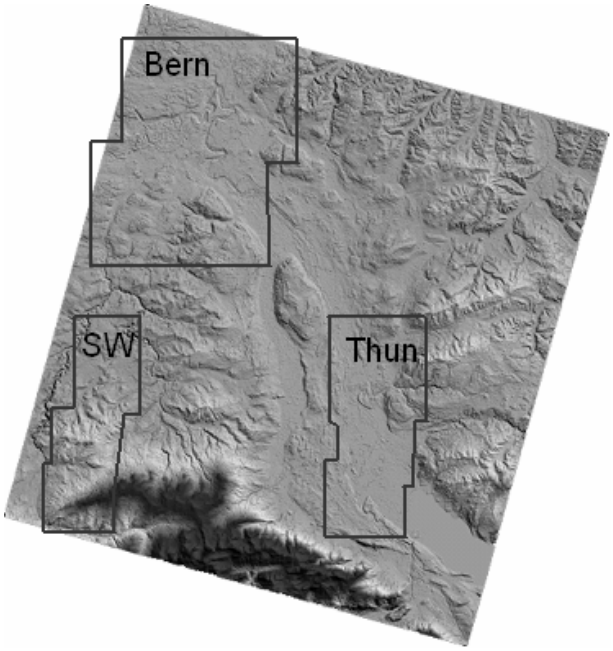

Figure 7. Shaded DSM of the Testfield Bern/Thun. The grid spacing is 5 m. The three smaller test areas for the validation of the DSM generation are marked. *Bern*: city and tree area, max. height difference 400m, *SW* (south west): mountainous and tree area, max. height difference 1500m, *Thun*: city, open and tree area, max. height difference 1000m.

Table 2 gives an overview of the DSM accuracy evaluation results. Each sub area contains more than 2.7 million points. The overall RMS height errors for all three test areas are better than three pixels (5.5 m – 6.6 m). As we expected, we get the best accuracy for open areas (O1, 4.7 m).
The worst results were obtained for a tree area next to a river, although a fairly wide area around the river was defined as dead area.

Figure 8 shows a part of the reference DSM (grid spacing 2.5 m) and the generated DSM (grid space 5m) in the city area of Bern. The main structure of streets and houses is visible in the generated DSM. Some bigger houses are easily detectable.

Table 2. DSM accuracy evaluation results of the three testareas Thun, SW (SouthWest) and Bern and for different sub-areas (O- Open areas, C – City areas, T – Tree areas, A – Alpine areas)

TF	*No. of points*	*$RMSE_Z$ [m]*	*Mean [m]*	*Min [m]*	*Max [m]*	*Z_{GEN} -Z_{REF} <5m*	*Z_{GEN} -Z_{REF} 5m-12.5m*	*Z_{GEN} -Z_{REF} 12.5m-25m*	*Z_{GEN} -Z_{REF} >25m*
Thun	**3508099**	**5.5**	**1.2**	**-41.6**	**63.4**	**75.6%**	**20.4%**	**3.7%**	**0.3%**
- O1	202704	4.7	1.1	-30.3	35.4	84.8%	12.2%	2.9%	<0.1%
- A2	291284	7.2	2.6	-33.8	61.3	74.7%	17.1%	7.2%	1.0%
SW	**2752822**	**6.6**	**0.55**	**-76.9**	**84.5**	**70.7%**	**23.6%**	**4.8%**	**0.9%**
- A1	815265	6.7	2.2	-46.4	80.0	74.0%	20.9%	4.6%	0.5%
- T1	80033	12.8	-1.8	-74.5	64.2	45.8%	32.4%	15.4%	6.4%
Bern	**4340836**	**5.7**	**-1.3**	**-60.0**	**50.0**	**70.8%**	**25.4%**	**3.5%**	**0.3%**
- C1	123954	5.6	-3.1	-74.6	70.9	97.2%	2.4%	0.3%	<0.1%
- C2	174464	5.0	-2.7	-28.5	27.8	98.0%	1.9%	0.1%	~0% (2)
- T2	126727	7.9	-2.9	-42.4	34.4	34.4	91.4%	7.4%	1.1%

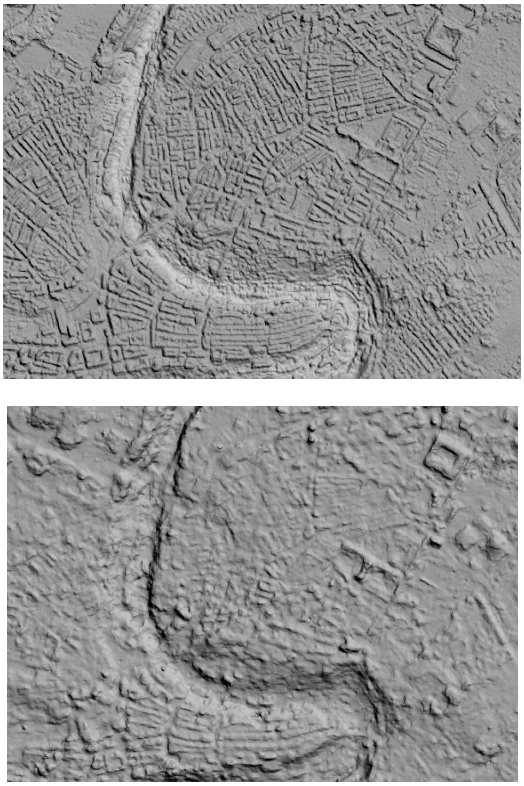

Figure 8. Shaded DSM of the city of Bern. Top: The reference DSM with a grid spacing of 2.5 m. Below: The generated DSM with a grid spacing of 5 m. The main structures of streets and houses are visible. Here the river was not defined as dead area.

4.2 Testfield Okazaki, Japan

The second testfield has been generated by JAXA and is located in the area of Okazaki, Japan. A given reference DSM (6 x 6 km ^{2}) in the southern part of the testfield consists mostly of forest and has been generated by using aerial images.
Table 3 gives the main parameters of the PRISM dataset acquired over the Okazaki testfield.
The generated DSM without any manual correction is shown in Figure 9. The grid spacing is again 5 m (2 pixels). For visualization we defined the lakes as dead areas (white holes in the DSM).

Table 3. Main parameters of the PRISM dataset acquired over the Okazaki testfield

Imaging date	June 20, 2006
Number of used GCPs	9
$RMSE_{XY}$ of selfcalibration (DGR)	1.9 m
$RMSE_Z$ of selfcalibration (DGR)	2.4 m

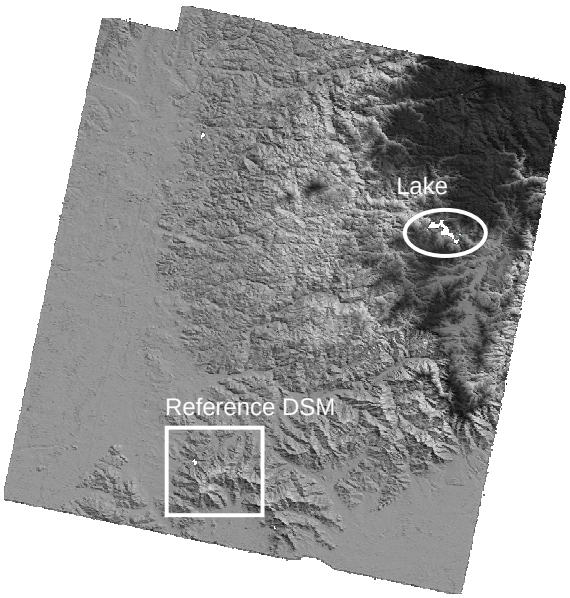

Figure 9. Shaded DSM of the testfield Okazaki. The grid space is 5 m. The white holes in the DSM are lakes, which are defined as dead areas. The reference DSM is located in the southern part of the testfield.

Table 4. DSM accuracy evaluation results of the sub area of the testfield Okazaki, Japan

No. of points	*$RMSE_Z$ [m]*	*Mean [m]*	*Min [m]*	*Max [m]*
388710	6.3	2.4	-102.4	99.6
Z_{GEN} -Z_{REF} <5m	*Z_{GEN} -Z_{REF} 5m-12.5m*	*Z_{GEN} -Z_{REF} 12.5-25m*	*Z_{GEN} -Z_{REF} >25m*	
64.9%	31.0%	3.5%	0.6%	

Table 4 gives an overview of the DSM accuracy evaluation results. The sub area with the reference DSM contains nearly 400 000 points. The RMS error of the height is better than three pixels (6.3 m).

5. CONCLUSIONS

We have validated the DSM generation using early ALOS/PRISM images over two testfields: Bern/Thun, Switzerland and Okazaki, Japan. The performance of PRISM imagery in connection with our multi-image matcher of SAT-PP was tested with three sub-areas of the Bern/Thun testfield and one in Okazaki.

The sub-areas of Bern/Thun were dominated either by city structure (Bern), mountainous areas (South-West) and midland (open fields, town, sparse trees (South-East, Thun)). Within these sub-areas we defined areas of specific and homogeneous topographic/land use characteristics (open space, city, trees, alpine) in order to test the DSM generation quality in dependence of these parameters. The height RMSE values ranged from 4.7 m (open areas) to 12.8 m (trees). This corresponds to a height accuracy of 2 – 5 pixels. The average values for the full sub-areas spanned from 5.5 to 6.6 m. All these values are based on the raw matching results, without any post-processing for blunder removal. There are still some blunders left in the data (up to 85 m), as can be seen from the histogram values of Table 2.

The sub area of Okazaki consists mostly of forest. The results of the DSM comparison are in the same range of the results of the testfield Bern/Thun.

If we compare these matching results with those which were obtained earlier with other satellite sensors of similar type (SPOT-5, IKONOS) we note that the accuracy (expressed in pixels) is about the same as with IKONOS, but less good than SPOT-5.

This is fully in line with our expectations and can be attributed to the differences in image configuration (PRISM was used in triplet mode, the others in stereo mode) on the one side and to the inferior image quality of PRISM on the other side.

But we believe that the concept of image triplets together with our multi-image matching approach would return for PRISM even better georeferencing and image matching results if only the radiometric image quality was better.

REFERENCES

Eisenbeiss H., Baltsavias E. P., Pateraki M., Zhang L., 2004. Potential of IKONOS and QUICKBIRD Imagery for Accurate 3D-Point Positioning, Orthoimage and DSM Generation. International Archives of Photogrammetry and Remote Sensing, 35 (B3), pp. 522-528.

Gruen A., Kocaman S., Wolff K., 2007. Calibration and Validation of Early ALOS/PRISM Images. The Journal of the Japan Society of Photogrammetry and Remote Sensing, Vol 46, No. 1, pp. 24-38.

Gruen A., Eisenbeiss H., Hanusch T., Sauerbier M., Wolff K., 2006. Documentation of the reference DSMs of the ALOS testfield Bern/Thun, Switzerland. Report to JAXA, Japan.

Gruen A., Zhang L., Esenbeiss H., 2005. 3D Precision Processing of High-Resolution Satellite Imagery. ASPRS 2005 Annual Conference, Baltimore, Maryland, USA, March 7-11, on CD-ROM.

Kocaman S., Gruen A., 2007. Orientation and Calibration of ALOS/PRISM Imagery. High-Resolution Earth Imaging for Geospatial Information, Proceedings of ISPRS Hanover Workshop 2007, to be published.

Zhang L., 2005. Automatic Digital Surface Model (DSM) Generation from Linear Array Images. PhD Dissertation, Mitteilungen Nr 88, Institute of Geodesy and Photogrammetry, ETH Zurich.

Zhang L., Gruen A., 2004. Automatic DSM Generation from Linear Array Imagery Data. International Archives of Photogrammetry and Remote Sensing, 35(B3), pp. 128-133.

Zhang L., Gruen A., 2006. Multi-image matching for DSM generation from IKONOS imagery. ISPRS Journal of Photogrammetry and Remote Sensing, Vol. 60, No. 3, pp. 195-211.